Talanta 130 (2014) 78–89

Contents lists available at ScienceDirect

Talanta

journal homepage: www.elsevier.com/locate/talanta

A nano-patterned self assembled monolayer (SAM) rutile titania cancer chip for rapid, low cost, highly sensitive, direct cancer analysis in MALDI-MS

M. Manikandan [a,b], Judy Gopal [a,b], Nazim Hasan [a], Hui-Fen Wu [a,b,c,d,e,*]

[a] Department of Chemistry, National Sun Yat-Sen University, Kaohsiung 70, Lien-Hai Road, Kaohsiung 80424, Taiwan
[b] Center for Nanoscience and Nanotechnology, National Sun Yat-Sen University, Kaohsiung 70, Lien-Hai Road, Kaohsiung 80424, Taiwan
[c] Doctoral Degree Program in Marine Biotechnology, National Sun Yat-Sen University, Kaohsiung 70, Lien-Hai Road, Kaohsiung 80424, Taiwan
[d] School of Pharmacy, College of Pharmacy, Kaohsiung Medical University, Kaohsiung 800, Taiwan
[e] Institute of Medical Science and Technology, National Sun Yat-Sen University, Lien-Hai Road, Kaohsiung 80424, Taiwan

ARTICLE INFO

Article history:
Received 28 March 2014
Received in revised form
14 June 2014
Accepted 17 June 2014
Available online 25 June 2014

Keywords:
Cancer chip
SAM
Titanium
Neuro 2A cells
Thermally oxidized
Mass spectrometry

ABSTRACT

We developed a cancer chip by nano-patterning a highly sensitive SAM titanium surface capable of capturing and sensing concentrations as low as 10 cancer cells/mL from the environment by Matrix Assisted Laser Desorption and Ionization Time of Flight Mass Spectrometry (MALDI-TOF MS). The current approach evades any form of pretreatment and sample preparation processes; it is time saving and does not require the (expensive) conventional MALDI target plate. The home made aluminium (Al) target holder cost, on which we loaded the cancer chips for MALDI-TOF MS analysis, is about 60 USD. While the conventional stainless steel MALDI target plate is more than 700 USD. The SAM surface was an effective platform leading to on-chip direct MALDI-MS detection of cancer cells. We compared the functionality of this chip with the unmodified titanium surfaces and thermally oxidized (TO) titanium surfaces. The lowest detectable concentration of the TO chip was 10^3 cells/mL, while the lowest detectable concentration of the control or unmodified titanium chips was 10^6 cells/mL. Compared to the control surface, the SAM cancer chip showed 100,000 times of enhanced sensitivity and compared with the TO chip, 1000 times of increased sensitivity. The high sensitivity of the SAM surfaces is attributed to the presence of the rutile SAM, surface roughness and surface wettability as confirmed by AFM, XRD, contact angle microscope and FE-SEM. This study opens a new avenue for the potent application of the SAM cancer chip for direct cancer diagnosis by MALDI-TOF MS in the near future.

1. Introduction

Since its discovery by William Gregor in 1791, titanium has expanded its horizons into multiple domains. Titanium is alloyed with iron, aluminum, vanadium, molybdenum, in order to produce strong lightweight alloys for use in aerospace (jet engines, missiles, and spacecraft), military, industrial (chemicals and petro-chemicals, desalination plants, pulp, and paper), automotive, agri-food and for applications such as medical prostheses, orthopedic implants, dental and endodontic instruments and files, dental implants, sporting goods, jewelry, mobile phones. Materials used for biomedical applications cover a wide spectrum and must exhibit specific properties. One of the vital requisite for the choice of an implant material is its biocompatibility and corrosion resistance properties. The major metallic biomaterials used frequently include, stainless steels, cobalt alloy, titanium and titanium alloys [1]. The biocompatibility of titanium is ascertained to the presence of the titanium oxide film. Therefore, researchers have focused their attention on the development of a stable oxide film on titanium surfaces to increase its biocompatibility [2–4].

Although the oxide film may play a direct or indirect role toward increasing the biocompatibility, it is possible that the factors such as roughness, hydroxyl group functionalization, type of oxide, hydrophobicity/hydrophilicity may play an equally indisputable role in this phenomenon [5]. The biocompatibility of titanium has a dark side when used as condenser material in power plants and in industries because it is prone to bacterial and

* Corresponding author at: Department of Chemistry, National Sun Yat - Sen University, Kaohsiung 70, Lien-Hai Road, Kaohsiung 80424, Taiwan.
Tel.: +886 7 5252000 3955; fax: +886 7 5253908.
E-mail address: hwu@faculty.nsysu.edu.tw (H.-F. Wu).

http://dx.doi.org/10.1016/j.talanta.2014.06.033
0039-9140/

microbial settlement (biofilm) on its surface, leading to a problem called biofouling. We [6–9] have previously reported the extensive microbial fouling property of titanium surfaces and their effective control by modulating the oxide properties.

MALDI technique was initially introduced by Hillenkamp [10] and then rapidly become an ideal (soft) ionization technique for the mass spectrometric analysis of biomolecules. Development of functionalized MALDI-MS targets platforms for probing analytes such as phosphopeptides, peptides, biomolecules and nucleic acids has been generously reported. Brockman and Orlando, used an antibody, lectin or receptor bound to the surfaces of the MALDI plates for probing weak cation-exchange focusing target solid-phase extraction/preconcentration [11]. Navare et al., used polymer films as MALDI probes [12] and Wang et al., immobilized immunoglobulins [13]. Neubert et al. used an affinity capture polymer [14]. Koopman and Blackburn, used a DNA aptamer covalently attached to the surface of a glass slide for ultrasensitive detection of hydrophobic proteins [15]. McComb, used silylated DIOS chip molecules and Trauger et al., a polymer thin film [16–18]. Torta et al. developed a nanostructured TiO_2 film coated on stainless steel plates for phosphopeptide enrichment [19]. Wang and Bruening [20] used silicon wafers. All these authors used various platforms for selective and sensitive capture of biomolecules for direct on-chip MALDI-MS detection. In the following paper we focus on describing the positive utilization of this inherent biocompatible property exhibited by titanium surfaces for the development of a titanium based cancer chip for direct on-chip detection of cancer cells using MALDI-MS. The cancer chips were surface modified to enhance the sensing ability by thermal oxidation and by nano patterning. This work reports and discuss the reasons the engineered surfaces show enhanced biocompatibility.

2. Materials and methods

2.1. Material

Titanium foil (0.5 mm thickness, 99% metal basis) was purchased from Alfa Aesar, Johnson Mathey Company, USA. Nitric acid (65%, reagent grade) from Scharlau chemie, Spain and hydrofluoric acid (48 wt% in water $\geq$99.99% trace metal basis) was bought from Sigma Aldrich, Germany. Acetone (99.99% analytical grade) was bought from, B.K baker, Germany. Double distilled water, purified by a Milli-Q reagent system (Millipore, Milliford, MA, USA) was used for each experiment.

2.2. Sample preparation

Commercially pure titanium grade-2 coupons (10 mm $\times$ 10 mm) were pickled in an acid bath containing 6.34 M nitric acid and 2 M hydrofluoric acid [8] and then ultrasonically cleaned using soap solution to remove all traces of acids from the surfaces. The chips were washed in running water and finally rinsed in distilled water and air dried. One set of these chips were retained as such prior to thermal oxidation and used as control (Fig. 1(a)) in this study. Fig. 1 gives the overall flow of work.

2.3. Heat treatment

The samples prepared as described above were subjected to thermal oxidation at 1000 °C for 3 h in a furnace (Thermo Scientific, Model no. FB1300, Dubuque, USA). The thermally oxidized metal chips were removed from the furnace after the specified period and air-cooled. A set of the thermally oxidized chips were retained as such, these are referred to as TO cancer chips in the subsequent text (Fig. 1(b)). The other set of the thermally oxidized chips were delaminated, since the oxide film could be detached easily from the metal surface by tapping (using a pair of forceps) on the corner of the chip. The oxide film detached as a fragile ivory white wafer from the surface (this delaminated oxide film was discarded), the underlying metal surfaces showed reminiscence of white deposits on the surface (Fig. 1(c)). We then subjected these surfaces to ultrasonication to rid the surface of any loosely adhering oxide particles. These delaminated chips are those that will be referred to as the SAM chips in the following manuscript. The control, TO and SAM chips were characterized using X-ray diffraction (XRD) (Bruker D8 advance, Germany), field emission scanning electron microscopy (FE-SEM) (Field Emission Scanning Electron Microscope, Jeol JSM-6700F, Japan), Atomic Force Microscope (AFM), Bruker, Nanoscope IV dimension 3100, Veeco Metrology Group and the surface hydrophobicity/hydrophilicity was measured using 'Pendant Drop Method' by contact angle microscope (OCA-20, USA).

2.4. Evaluating the capture efficiency/sensor ability of cancer chips

Mouse Neuroblastoma cell line Nero2A CCL-131 was purchased from American Type Culture Collection (Rockville, MD). Neuro 2A cells were cultured in a flask containing Minimum Essential Eagle's Medium (MEM) supplemented with 10% heat-inactivated FBS and 1% streptomycin/penicillin (Invitrogen). The flask was placed in a humidified atmosphere with 5% CO_2 at 37 °C in a cell culture incubator (Sanyo Inc, Japan). The cells were trypnized by Trypsin—EDTA (25% V/V) for 5 min in order to make a uniform suspension. The cell count was enumerated using the Haemocytometer (Marienfeld, Germany) under an inverted ESPA FI40 microscope (NIB-100F, ESPA systems Co. Ltd., Taiwan). The biochips were exposed to 6 different cell concentrations such as 1×10^6, 1×10^5, 1×10^4, 1×10^3, 1×10^2 and 1×10^1 cells/mL in a 6-well plate (Fig. 1). The chips were retrieved at 3 h, 6 h and 20 h after exposure to the cells and rinsed in PBS solution prior to epifluorescence and MALDI-MS analysis.

2.5. Post exposure analysis using epifluorescence microscope and SEM

The chips were gently rinsed with PBS solution and air dried in a sterile chamber and their surface was flooded using acridine orange (0.1% solution in distilled water). After 10 min, the excess stain was drained off and the TBC's were washed in sterile water, dried and observed. Acridine orange, a fluorescent dye, differentially stains single stranded RNA and double stranded DNA. Acridine orange, fluoresces orange when intercalated with the former and green while complexing with the latter when observed under an ESPA FI40 (NIB-100F, ESPA systems Co. Ltd., Taiwan) inverted epifluorescence microscope (excitation filter BP 490; barrier filter O 515) [7]. Chips exposed to cancer cells (10^4 cells/mL) for 6 h were retrieved and prepared for FE-SEM analysis. The cells required to be fixed and dehydrated prior to FE-SEM analysis. The cancer cells attached to the control, TO and SAM cancer chips were fixed in 2.5% glutaraldehyde for 3 h, after that the surfaces were rinsed using phosphate buffer, followed by incubation with osmium tetroxide for 1 h. The chips were process through an ethanol series ranging from 20% to 100% for dehydration and dried *invacco* overnight prior to FE-SEM analysis.

2.6. Detection of captured cancer cells by direct on-chip MALDI-MS

After retrieving the chips from the solution (after 3 h, 6 h and 20 h), the chips were gently rinsed with sterile water and air dried in a sterile chamber. Then the surface was loaded with about 50 μL

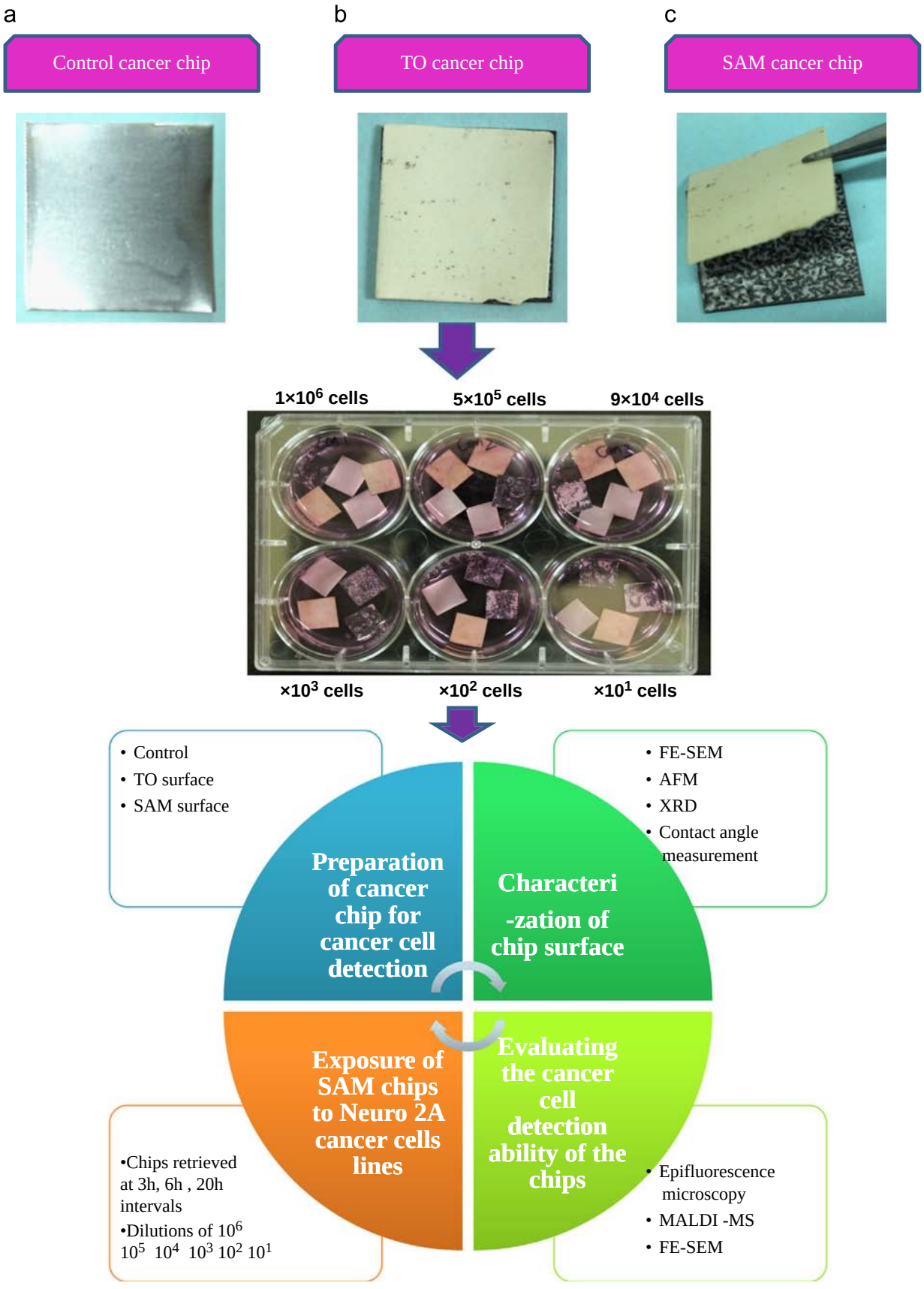

Fig. 1. Schematic showing of work flow followed in this paper.

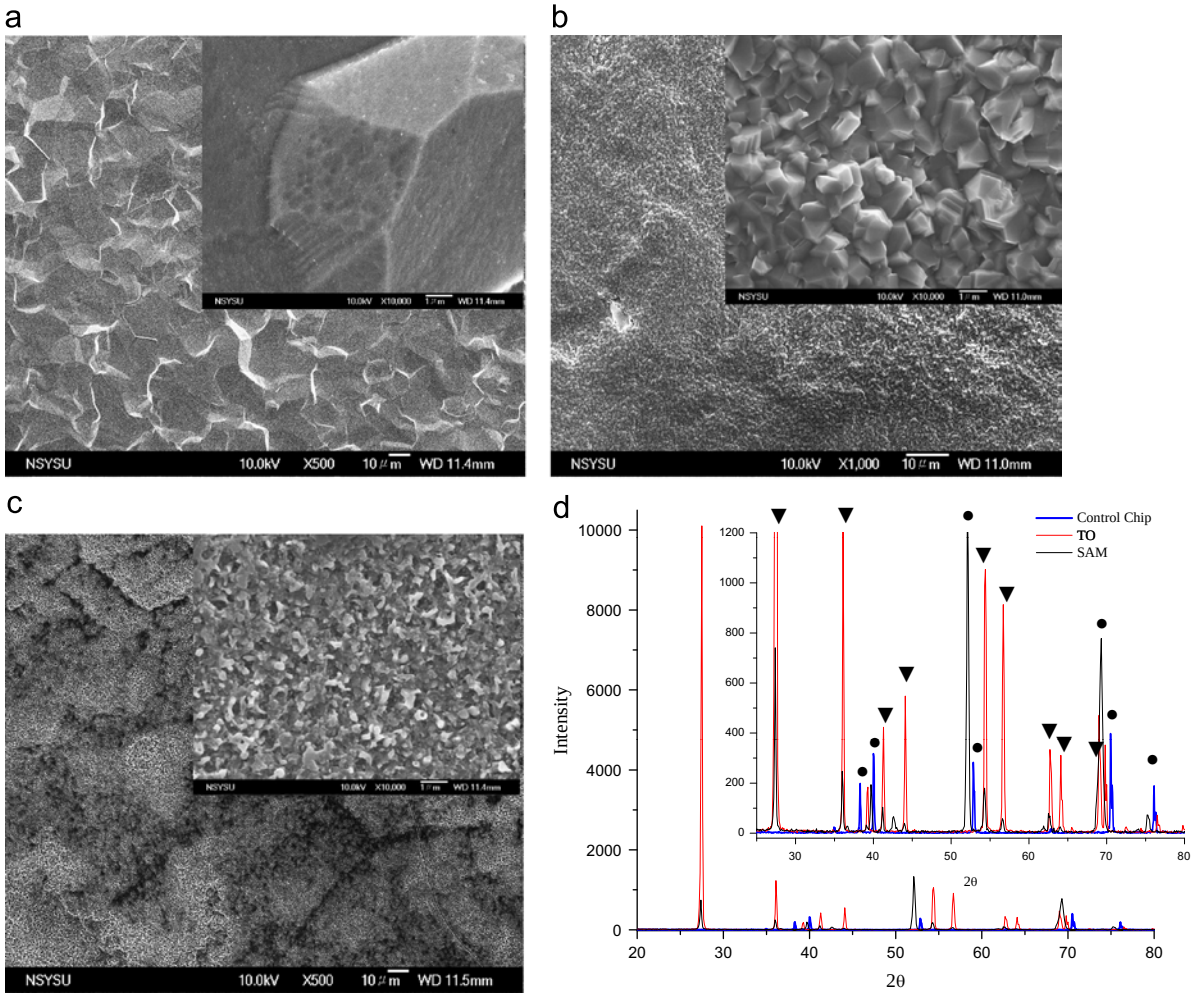

Fig. 2. FE-SEM images of (a) control surface (b) TO surface and (c) SAM cancer sensor surface, inset shows 1 μm scale magnified images of the respective surfaces (d) XRD graph showing surface characteristic of control, TO chip and SAM chip. The symbol • represents Ti peaks and ▾represents rutile peaks.

of 50 mM SA matrix (0.05 M sinapinic acid (SA) in 3:1 Acetonitrile: Water containing 0.1% TFA) and air dried before analyzing the TBC's using MALDI-MS. All mass spectra were obtained in positive ion mode using a MALDI-TOF MS (Microflex, Bruker Daltonics, Bremen, Germany). The MALDI source was equipped with a nitrogen laser (337 nm) for sample irradiation and the accelerating voltage was set at +20 kV. All experiments were performed in the linear mode using optimal laser energy.

3. Results and discussion

3.1. Characterization of cancer chips

3.1.1. FE-SEM

The surfaces of the three cancer chips were characterized using FE-SEM. The three cancer chips showed distinct morphologies. Fig. 2(a) gives the FE-SEM micrograph of the control cancer chip, as can be observed the chip surface reveals the natural oxide film present on the titanium surface. Since these surfaces were not thermally oxidized, the oxide film is rather thin; this can be assumed from the fact that we are able to see the grain boundaries of the underlying metal surface, implying that the film is not thick. It is reported [21–24] that this natural oxide film formed on the titanium surface is around 30–80 Å thick and it increases upto 250 Å with increasing exposure to air for 4 years. The inset shows the magnified view of the control chip surfaces. The total disappearance of the grain boundaries in Fig. 2(b) shows that the oxide film has gained considerable thickness on the thermally oxidized chip surface. Thermal oxidation at high temperatures similar to that was used in this study, i.e. 1000 °C, leads to the formation of a visible ivory colored oxide film almost 1–2 mm in thickness. The inset in Fig. 2(b) indicates that this film is well structured into 0.5–1 μm TiO_2 crystalline particles, compactly organized on the titanium surface. This film was brittle and had to be handled with care. Fig. 2(c) gives the appearance of the SAM surface underlying the delaminated oxide film. As observed, this surface was highly porous and showed 200–500 nm sized webbed particles, whose arms interconnected to form a porous network. The thermally oxidized surface and the SAM surface after delamination of oxide film were distinctly different and had unique morphologies.

3.1.2. XRD

Fig. 2(d) gives the XRD graph showing the peaks obtained on the control, TO and SAM surface. As can be observed from the graph, the control surface shows the presence of solely titanium peaks. The TO surface show peaks corresponding to that of rutile titania. XRD patterns exhibited strong diffraction peaks at 27°, 36° and 54° indicating TiO_2 in the rutile phase. All peaks are in good agreement with the standard spectrum available at JCPDS no.: 88-1175 for rutile [25]. It was interesting to note that the entire spectrum of pure rutile titania peaks were observed in addition to

the 100, 50 and 60 peaks observed at 27°, 36° and 54°, respectively. These results suggest that at thermal oxidation temperatures as high as 1000 °C, a complete transformation into rutile results. We did not observe any titanium peaks, obviously because the oxide film was thick and completely masked the substrate effect. On the SAM surface, it was interesting to observe that we still obtained the rutile peaks. However, the intensity was significantly decreased (741 counts/s) than the peak observed on the TO surface (10,073 counts/s). The smaller and broader nature of this peak also suggests the differences in the crystallinity of the rutile film on these surfaces. It is possible that the SAM rutile film on the SAM surface is amorphous. Also, minor shifts in the peak values were observed on the SAM surface, which also suggests that the nature of this SAM layer is not very similar to the rutile oxide film which forms by thermal oxidation. We could also observe a few titanium peaks suggesting the porous nature of the film on the surface. This also suggests that this self- assembled monolayer was rather thin and its major composition was rutile. Since the parent oxide film had been delaminated it was uncertain what the underlying SAM layer on the titanium surface was made up of. These studies clearly show that the SAM layer was indeed rutile titania. Previous work [26] also reports the SAM layer underlying the delaminated rutile oxide film being rutile.

3.1.3. AFM

The control, TO and SAM cancer chips were characterized using AFM. The results showed that the morphology of these surfaces were apparently different. Fig. 3 gives the AFM 3-D images of control (a and b), TO chip (c and d), SAM (e and f) chip surfaces. The roughness of these surfaces was measured based on offline analysis of the AFM images. The mean roughness (R_a) of the surface was obtained from three different areas on the same chip. Table 1 shows the average roughness values for the control (13.152 nm), TO chip (32.984 nm) and SAM surface (84.763 nm). Based on these results it can be observed that the SAM surface showed the highest roughness compared to the TO surface and least roughness was observed on the control surfaces. Later we would discuss the importance of roughness as a function of the enhanced cell capture shown by the respective surfaces.

3.1.4. Contact angle measurement

The contact angles of the three chip surfaces were measured using contact angle measurement microscope (Table 1). Fig. S1 gives the snapshot of the water drop on the control (a), TO (b) and SAM cancer (c) chip surfaces. The more the spread of the water drop, the more is the hydrophilicity of the surface. Based on this inference, the TO surfaces appear to show the highest wettability (hydrophilicity), followed by the SAM surface and then the control surface. The contact angles measured also confirmed this observation, the table indicates that the control cancer chip surfaces were near-hydrophilic with a contact angle of 62°, the TO surface had a superhydrophilic surface with an average contact angle of 25° and the SAM surface has a near-superhydrophilic surface with contact angle 39°. These studies also indicated that the three test surfaces exhibited distinct wettability properties. The relevance of these properties in the effective functioning of these chips has been discussed later in the manuscript.

3.2. Evaluating the cancer sensing ability

The ability of the cancer chips to capture the cancer cells from the surrounding medium was evaluated at three time intervals, namely 3 h, 6 h and 20 h. The control, TO chip and the SAM chips were retrieved at these specific time intervals and the captured cancer cells were detected by direct MALDI-MS. It was observed that the control and TO cancer chips did not show much peaks (Fig. 4(a) and (b)) at cell dilutions of 10^4 cells/mL, however the SAM chip surface (Fig. 4(c)) gave significant cancer protein signals, indicating that even as early as 3 h the SAM chips were able to capture cancer cells onto their surface and lead to effective detection by MALDI-MS. The control surfaces did capture and detection at 3 h when exposed to high concentration of cells, such as 10^6 cells/mL and 10^5 cells/mL. Fig. S2A reveals this fact, cancer signals were observed at 10^6 cells/mL (Fig. S2A(a)) and 10^5 cells/mL (Fig. S2A(b)) concentrations but no signals were observed at lower dilutions of 10^4 cells/mL (Fig. S2A(c)). In the case of the TO cancer chip, it was observed that the 10^6cells/mL (Fig. S2B(a)) and 10^5cells/mL (Fig. S2B(b)) concentrations yielded good signals, but the signals reduced to a large extent at lower dilutions of 10^4 cells/mL (Fig. S2B(c)). Thus, it can be concluded that the control chip was effective only at high cell concentrations as early as 3 h, the TO chips surfaces also appeared less effective at 10^4 cell/mL concentrations. The Epifluorescence detailed studies of the chip surfaces at 3 h, 6 h and 20 h intervals gave an insight into the capture efficiency of these surfaces. Fig. S3 shows the micrographs revealing the cell attachment on the control (a–c), TO (d–f) and SAM (g–i) surfaces at 3 h. The microscopic observation too supports the fact that the SAM surfaces showed enhanced capture at all dilutions. However, it was also observed that the control (Fig. S4 (a–c)) and TO (Fig. S4(d–f)) chips were able to detect upto 10^4 cell dilutions after longer incubation beyond 6 h. Fig. 5 gives the epifluorescence of micrographs showing cancer cell attachment on the control, (a–c), TO (d–f) and SAM (g–i) surfaces after 20 h incubation. In spite of prolonged incubation as long as 20 h, the control (Fig. 5(c)) and TO (Fig. 5(f)) surfaces showed minimal attachment at 10^4 cell/mL concentrations. From all these microscopic and MALDI-MS evidences, it can be summarized that the SAM surfaces were effective even as early as 3 h in sensoring the cancer cells in the surrounding medium and leading to detection using MALDI-MS. While the control and TO surfaces were operational only at high concentration for lesser incubation time (3 h) and for lower concentration (upto 10^4 cells/mL) they required more time (>6 h). Thus, the SAM chip could lead to early detection of cancer cells as early as 3 h. Based on these informations, we followed 6 h exposure time for the preceding experiments to suit the requirement of all the three test surfaces. The FE-SEM studies too confirmed that compared to the control (Fig. S5(a)) chip and the TO chip (Fig. S5(b)), the SAM chip (Fig. S5(c)) showed significant cells number on its surface. The FE-SEM sample preparation consists of a series of fixation and dehydration and washing protocols, the cells that remain on the surface are those that were really adherent to the surface. Although the TO chip shows more cells in the epifluorescence studies, it appears that the adherence of the cells was not much, this could have lead to their detachment from these surfaces during FE-SEM sample preparation. On the other hand, the SAM chips showed significant cell numbers, confirming that the cell-surface interaction on these surfaces was high.

3.3. Evaluating the lowest detectable concentration of cancer chips

The control, TO and SAM cancer chips were exposed to various concentrations of cancer cells ranging from 10^6, 10^5, 10^4, 10^3, 10^2, 10^1 cells/mL and retrieved after 6 h in order to determine the lowest detectable concentration of the three cancer chips using MALDI-MS. With respect to the control chips (Fig. 6A) it was observed that the cell concentrations of 10^6 cells/mL showed substantially good cancer signals (Fig. 6A(a)) beyond that 10^5 (Fig. 6A(b)) and 10^4 (Fig. 6(c)) concentrations showed just two peaks and beyond 10^4 no signals could be obtained from these surfaces. From the TO surface (Fig. 6B(a–d)), it was observed that

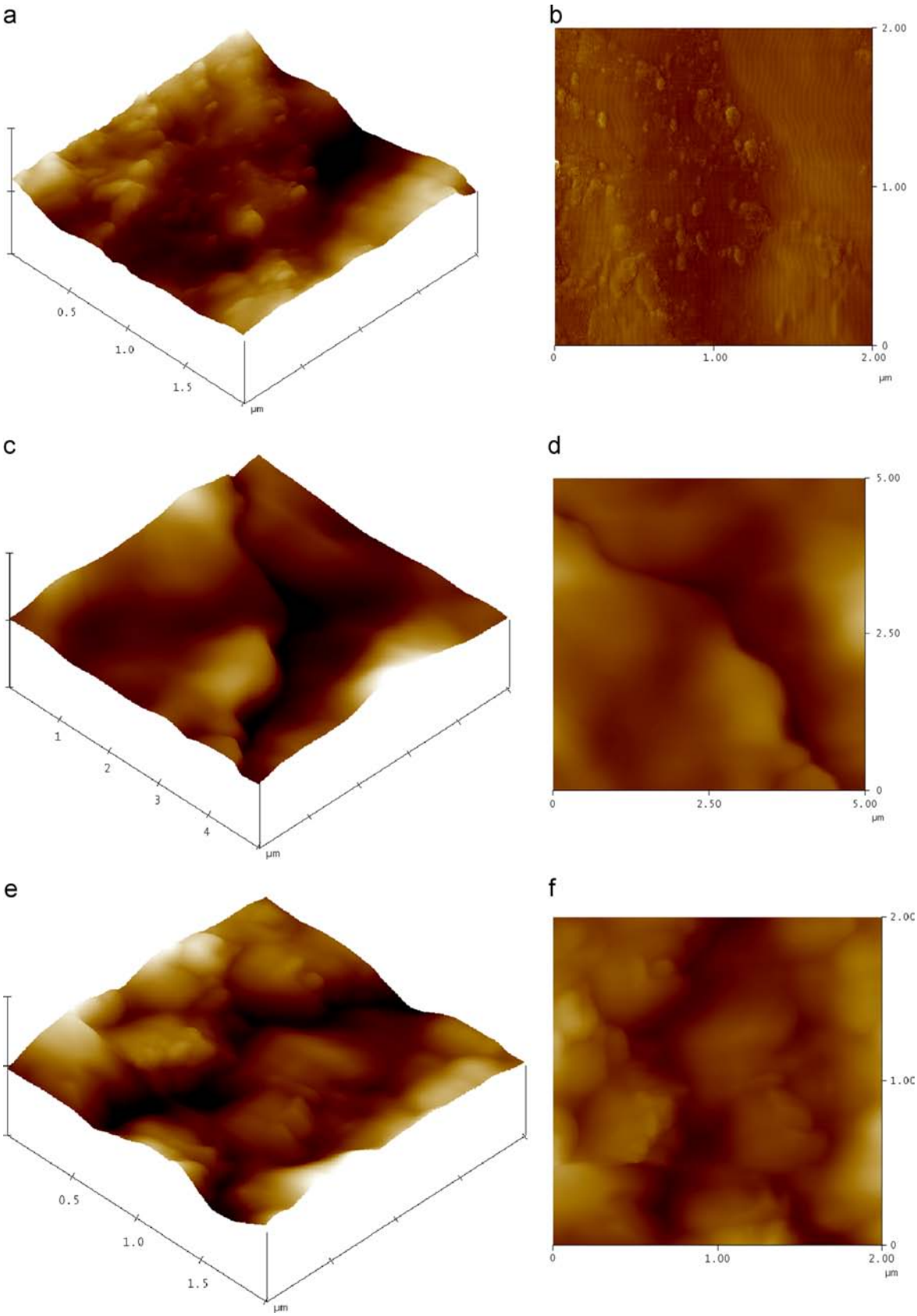

Fig. 3. AFM images of control (a) 3-D and (b) 2-D images; TO (c) 3-D and (d) 2-D images and SAM chip (e) 3-D and (f) 2-D images.

upto 10^3, good signals were obtained, the signals on the TO surface were more frequent and obtained at almost every hit on the chip surface. Thus, it can be surmised that 10^6 cells/mL were the lowest detectable concentration using control chips and 10^3 cells/mL was the lowest detectable concentration in case of the TO cancer chips. Fig. 7 gives the results of the spectra obtained from the SAM

Table 1
Surface hydrophobicity/hydrophilicity and roughness of the test surfaces.

BC-code	Left side CA (°)	Right side CA (°)	Average (°)	(Hydrophobicity/hydrophilicity)	Roughness (AFM probe)	Average (nm)
Control	59.4	59.1	62	(Near-hydrophilic)	13.993	13.152
	56.8	59.3			15.341	
	69.6	68.0			10.123	
1000° C	16.3	16.3	25	(Superhydophilic)	20.991	32.984
	38.5	28.2			46.718	
	26.7	26.7			31.243	
SAM	39.7	41.3	39	(Near-superhydrophilic)	99.751	84.763
	39.1	46.3			63.193	
	35.8	35.8			91.345	

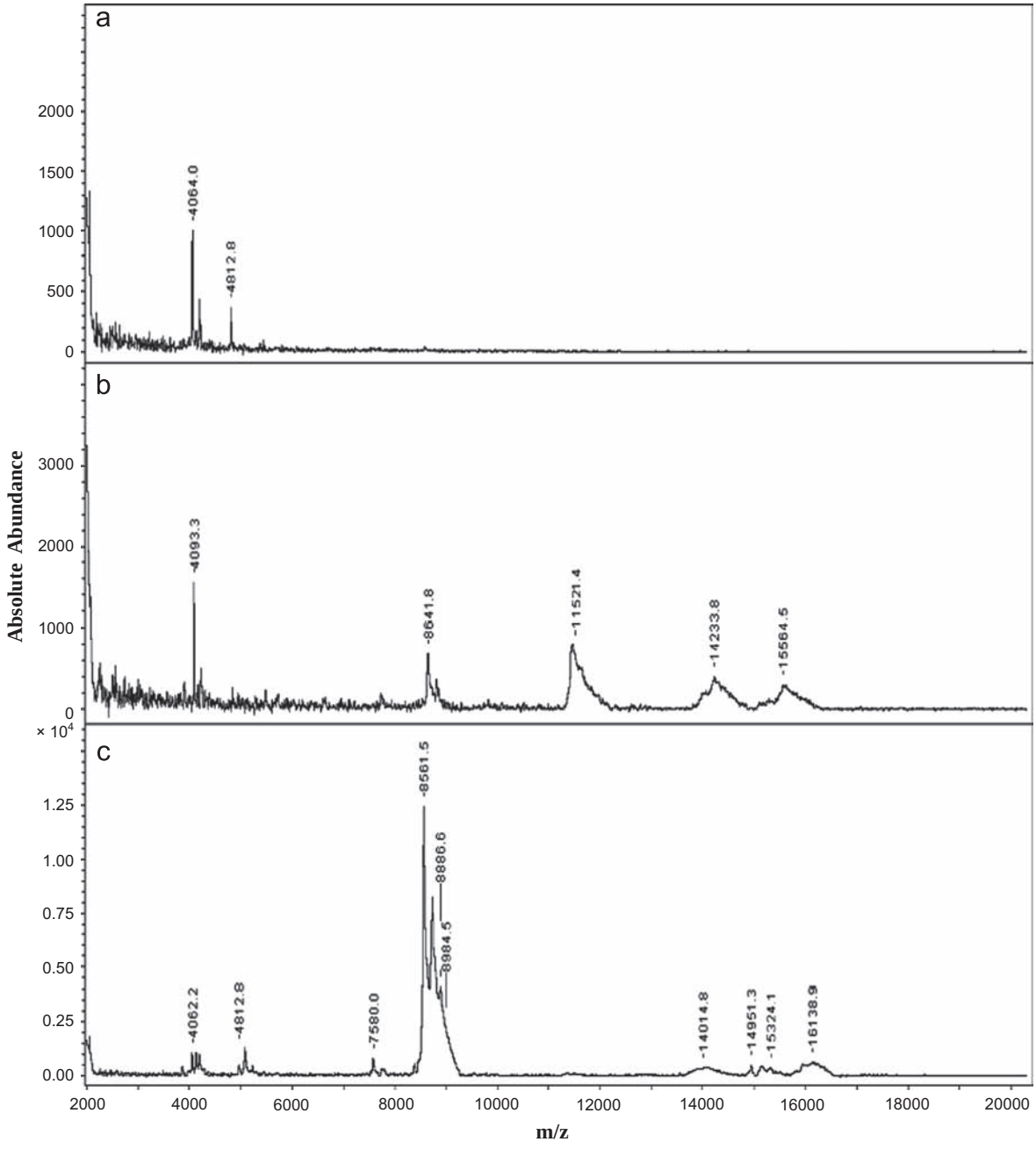

Fig. 4. MALDI-MS spectra showing the comparative cancer cell capture efficiency of the (a) control (b) TO and (c) SAM cancer chip surface after a minimal exposure time of 3 h.

cancer chips exposed to 10^6 (Fig. 7(a)), 10^5 (Fig. 7(b)), 10^4 (Fig. 7(c)), 10^3 (Fig. 7(d)), 10^2 (Fig. 7(e)) and 10^1 (Fig. 7(f)) cells/mL concentrations. The SAM chips showed significant cancer signals at all concentrations and showed a significant detectable concentration threshold at 10 cells/mL. Thus, the SAM surface was found to possess early sensoring ability (< 3 h) and also a sensitive

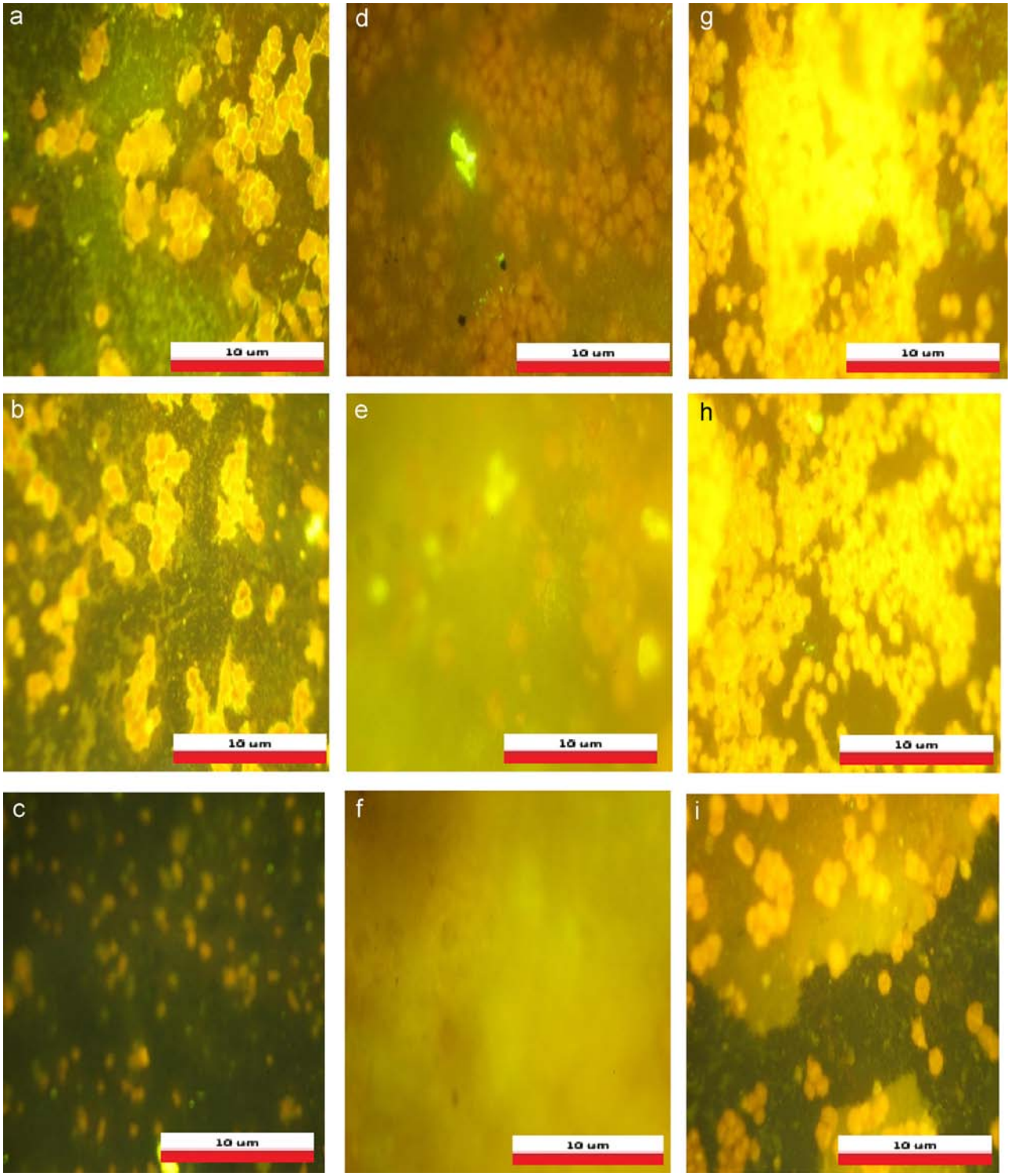

Fig. 5. Epifluorescence microscopic images of control surfaces exposed to (a) 10^6 (b) 10^5 (c) 10^4 cells/mL of cancer cells; TO surfaces exposed to (d) 10^6 (e) 10^5 (f) 10^4 cells/mL of cancer cells and SAM surfaces exposed to (g) 10^6 (h) 10^5 (i) 10^4 cells/mL of cancer cells for 20 h. Scale bar = 10 μm.

detection threshold concentration of 10 cells/mL surpassing both the control and TO chips in wither properties. Also, in terms of stability, the TO cancer chips had a highly fragile oxide film, which got detached easily and hence was not a suitable chip in terms of stability. From all these studies we conclude the SAM surface as the potent cancer chip leading to effective capture and detection using mass sensors.

Titanium is a naturally biocompatible material and is being widely used as medical implant material. Titanium is one of the most versatile new age materials and is used in various industries owing to its high-strength to weight ratio. It is highly corrosion resistant and resistant to even highly corrosive acids. Thus, when it is applid as a MALDI target plate, its mechanical properties and long periods for use will be unquestionable. We have previously studied the extensive microbial fouling property of titanium surfaces [7–9] and their effective control by modulating the oxide properties. There are other authors who report the increase in bioactivity of the titanium surface with heat treatment [27].

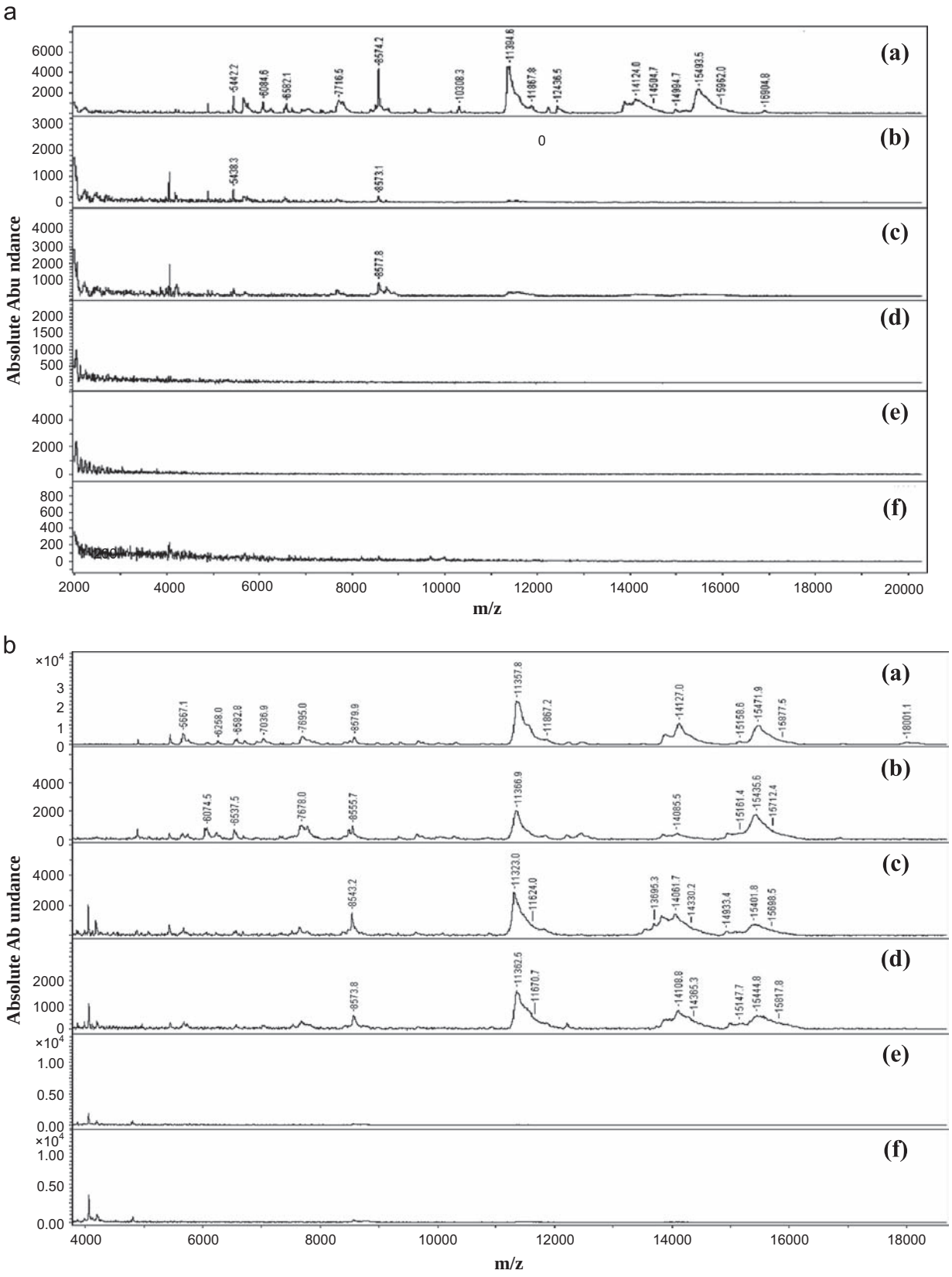

Fig. 6. (A) MALDI-MS spectra acquired by direct on-chip analysis of control surfaces exposed to (a) 10^6 (b) 10^5 (c) 10^4 (d) 10^3 (e) 10^2 (f) 10^1 cells/mL of neuro 2A cancer cells for 6 h. (B) MALDI-MS spectra acquired by direct on-chip analysis of TO cancer chip surfaces exposed to (a) 10^6 (b) 10^5 (c) 10^4 (d) 10^3 (e) 10^2 (f) 10^1 cells/mL of neuro 2A cancer cells for 6 h.

Still other authors reported that the surface biocompatibility of titanium can be greatly improved by surface modification [28,29]. All these studies explain the reason why the TO titanium surfaces and even the control titanium surfaces show affinity for capturing cancer cells. Surface roughness is yet another factor which has been reported to significantly enhance the adhesion of biological

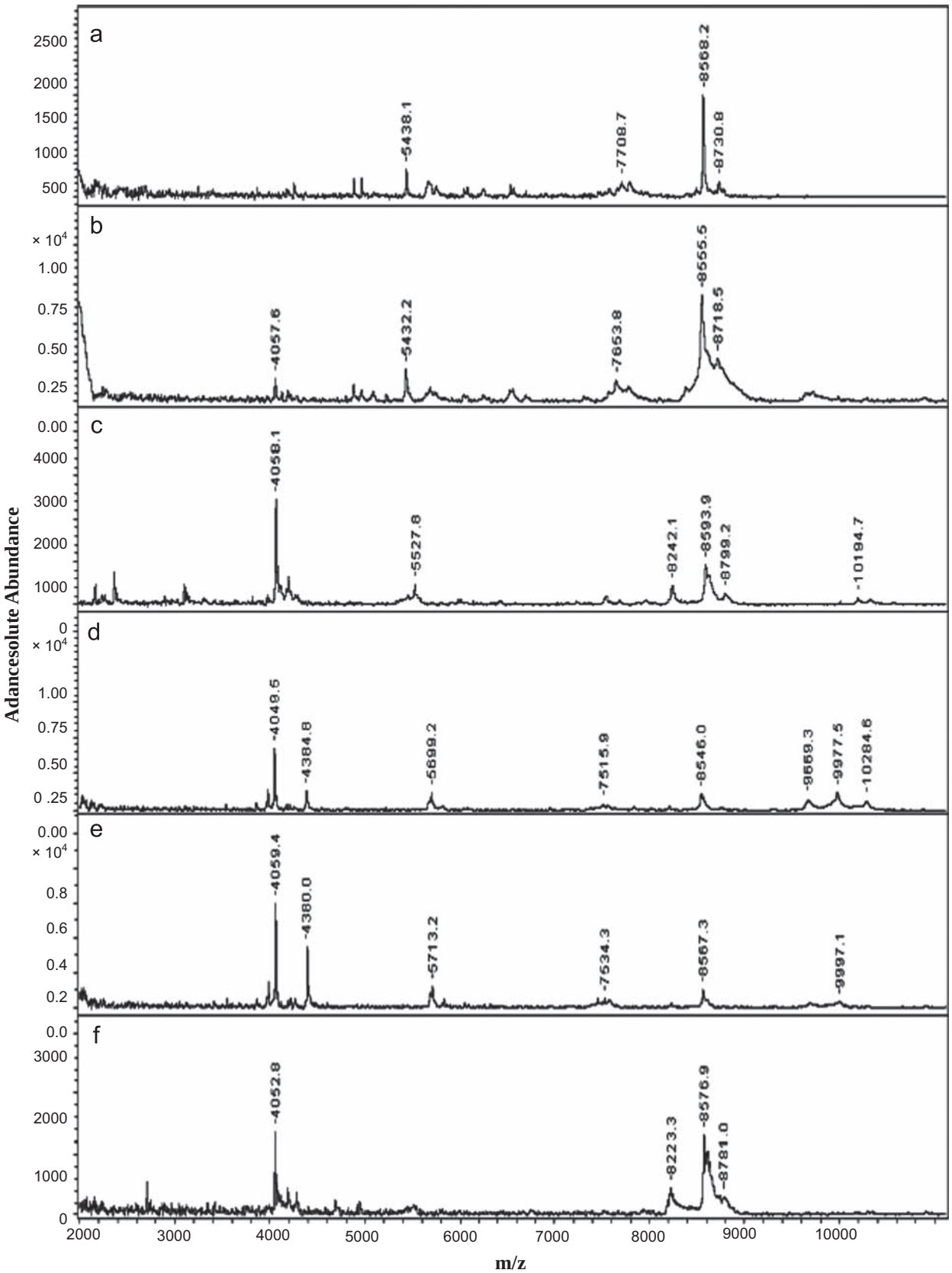

Fig. 7. MALDI-MS spectra acquired by direct on-chip analysis of SAM cancer chip surface exposed to (a) 10^6 (b) 10^5 (c) 10^4 (d) 10^3 (e) 10^2 (f) 10^1 cells/mL of neuro 2A cancer cells for 6 h.

cells to titanium surfaces by Gopal et al. [9]. Thus it appears that a large number of factors may play a role in the biocompatibility of titanium.

It is possible that the biocompatibility or cancer cell sensor ability of the three different chips used in this study may depend on independent factors. The control surfaces which were

unmodified titanium surfaces also show a certain degree of capture efficiency, this is most probably due to the fact that the titanium is a biocompatible material that does not release any toxic ions and hence is a favorable substrate for attachment of living cells. The control surface as demonstrated by the contact angle measurements is a near hydrophilic surface and this is also a factor which governs cell attachment to these surfaces. The thermally oxidized (1000 °C) titanium surface has an oxide film formed at high temperature. Feng et al. [27] have reported the increase of bioactivity (with respect to biological tissues) of titanium surfaces as a consequence of heat treatment. They report that rutile TiO_2 forms at higher temperatures and leads to enhanced cell adhesion. During heating treatment, oxygen and water react with the titanium surface, increasing the amount of hydroxyl groups on the surface besides leading to thickening of the oxide film. The presence of a hydrated oxide film with more –OH groups is reported to favor cell adhesion [30,31]. From a chemical thermodynamic standpoint, the formation of rutile TiO2 is reported [27] to be a favorable process, since the Gibbs function of rutile formation (-888.67 kJ mol^{-1}) is lower than that of anatase. Previous authors [32,33] report the existence of basic hydroxyl groups $(OH)_b$, acidic hydroxyl groups $(OH)_a$ and surface hydroxyl groups on rutile thin films which make the titanium surface extremely bioactive. Moreover, the TO surface was found to be super hydrophilic. This is a factor that would greatly influence cell adhesion. A combination of surface wettability and surface hydroxyl groups could be operational on the TO cancer chips. Also, the effect of surface energy on biological properties is a well documented fact [34]. Feng et al. reported that they had observed that heat treatment increased the surface energy of titanium. This was attributed to the change of the surface composition and the increase in the specific surface area occurring as a consequence of heat treatment. The control titanium surface or the non-thermally oxidized surface would according to their perspective have lower surface energy compared to the TO cancer chip and the SAM cancer chip. In case of the SAM cancer chips it is possible that the surface near-superhydrophilic property of this surface and also the surface roughness play a key role in the enhanced capture efficiency of these surfaces [35–37].

Kazuya et al. report that the delamination of the oxide film leaves a underlying self-assembled monolayer of rutile which for their heat treatment conditions was superhydrophilic and rough [26]. The AFM studies confirmed that the SAM surfaces showed more surface roughness compared to the control and TO surfaces. Also it was interesting to note that the cell capture was efficiency was also in the same order as that of surfaces roughness SAM > -TO > control. Thus, roughness does appear to play a vial role in the surface bioactivity of the chips. Moreover, our XRD studies also confirmed that the delamination of the oxide film left a self assembled layer of rutile on the chip surface. It is possible that this SAM layer of rutile exhibits varying properties than the parent rutile film (delaminated layer). The morphology of this SAM rutile film was distinctly different from the parent rutile film as exposed by our AFM and FE-SEM. The wettability properties and the nature of the oxide film as shown by contact angle measurements and XRD analysis also depict that these two oxide films were distinct. The removal of the parent oxide film, leaving behind the SAM surface could make this virgin surface highly reactive, leading to the enhanced capture efficiency demonstrated by this chip. The TO chip also showed significant capture efficiency compared to the control, with a lower detectable concentration of 10^3 cells/mL. But the SAM surface showed an incredibly higher detection limit of 10 cells/mL which we can say is owing to the unique combination of all the factors that made the TO chip along with the additional presence of the SAM porous rutile nanopatterned surface.

4. Conclusion

We report the development of a SAM rutile nanopatterned film by a two step process involving thermal oxidation followed by delamination the oxide film from titanium surfaces. These SAM cancer chips were able to detect cancer cells at extremely low cell concentration as 10 cells/mL by MALDI-MS. The lowest detectable concentration in case of TO chip surface was 10^3 cells/mL and control, 10^6 cells/mL. The vital attributes leading to the enhanced sensitivity of this chip include a combination of properties such as surface roughness, surface wettability and surface energy of the SAM rutile film on these cancer chips. The SAM chip hold an excellent future for capture of cancer cells from surrounding media followed by direct on-chip MALDI-MS analysis.

Acknowledgement

We thank and greatful to the Ministry of Science and Technology of Taiwan for financial support.

Appendix A. Supporting information

Supplementary data associated with this article can be found in the online version at http://dx.doi.org/10.1016/j.talanta.2014.06.033.

References

[1] T. Yasunaga, F. Kamikubo, N. Kitagawa, Y. Ito, T. Ogawa, T. Saito, S. Ono, K. Ajito, T. Minabe, K. Hashimato, A. Fujishiama, Titanium'95: Science & Technology Volume II—Proceedings Eighth World Conference Titanium, in: P A Blenkinsop, W J Evans, H M Flower (Eds.), The Institute of Materials, UK, 1996, pp. 1879–1885.
[2] P. Li, C. Ohtsuki, T. Kokubo, K. Nakanishi, N. Soga, K. de Groot, J. Biomed. Mater. Res. 28 (1994) 7–15.
[3] C. Ohtsuki, H. Iida, S. Hayakawa, A. Osaka, J. Biomed. Mater. Res. 35 (2004) 39–47.
[4] B. Liang, S. Fujibayashi, M. Neo, J. Tamura, H.M. Kim, M. Uchida, T. Kokubo, T. Nakamura., Biomaterials 24 (2003) 4959–4966.
[5] B. Feng, J.Y. Chen, S.K. Qi, L. He, J.Z. Zhao, X.D. Zhang., J. Mater. Sci. Mater. Med. 13 (2002) 457–464.
[6] J. Gopal, R.P. George, P. Muraleedharan, S. Kalavathi, S. Banerjee, H.S. Khatak., J. Mater. Sci. 42 (2007) 5152–5158.
[7] J. Gopal, R.P. George, P. Muraleedharan, H.S. Khatak., Biofouling 20 (2004) 167–175.
[8] J. Gopal, P. Muraleedharan, H. Sarvamangala, R.P. George, R.K. Dayal, B.V.R. Tata, H.S. Khatak, K.A, Biofouling 24 (2008) 275–282.
[9] J. Gopal, B.V.R. Tata, R.P. George, P. Muraleedharan, R.K. Dayal., Surf. Eng. 24 (2008) 447–451.
[10] M. Karas, D. Bachmann, U. Bahr, F. Hillenkamp, Int. J. Mass Spectrom. Ion Processes 78 (1987) 53–68.
[11] A.H. Brockman, R. Orlando, Rapid Commun. Mass Spectrom. 10 (1996) 1688–1692.
[12] A. Navare, M. Nouzova, F.G. Noriega, S. Hernández-Martínez, C. Menzel, F.M. Fernández, Rapid Commun. Mass Spectrom. 23 (2009) 477–486.
[13] H. Wang, K. Tseng, C.B. Lebrilla, Anal. Chem. 71 (1999) 2014–2020.
[14] H. Neubert, E.S. Jacoby, S.S. Bansal, R.K. Iles, D.A. Cowan, A.T. Kicman, Anal. Chem. 74 (2002) 3677–3683.
[15] J.O. Koopmann, J. Blackburn, Rapid Commun. Mass Spectrom. 17 (2003) 455–462.
[16] M.E. McComb, D.H. Perlman, H. Huang, C.E. Costello, Rapid Commun. Mass Spectrom. 21 (2007) 44–58.
[17] S.A. Trauger, E.P. Go, Z. Shen, J.V. Apon, B.J. Compton, E.S.P. Bouvier, M.G. Finn, G. Siuzdak, Anal. Chem. 76 (2004) 4484–4489.
[18] M. Li, R.B. Timmons, G.R. Kinsel, Anal. Chem. 77 (2005) 350–353.
[19] F. Torta, M. Fusi, C.S. Casari, C.E. Bottani, A. Bachi, J. Proteome Res. 8 (2009) 1932–1942.
[20] W.H. Wang, M.L. Bruening, Analyst 134 (2009) 512–518.
[21] E. McCafferty, J.P. Wightman., Surf. Interface Anal. 26 (1998) 549–564.
[22] E. McCafferty, J.P. Wightman, T.F. Cromer., J. Electrochem. Soc. 146 (1999) 2849.
[23] Z. Tun, J.J. Noël, D.W. Shoesmith., J. Electrochem. Soc. 146 (1999) 988–994.
[24] V.V. Andreeva., Corrosion 20 (1964) 35–46.
[25] K. Thamaphat, P. Limsuwan, B. Ngotawornchai., Kasetsart J. (Nat. Sci.) 42 (2008) 357–361.

[26] N. Kazuya, N. Shunsuke, Y. Yumi, O. Tsuyoshi, M. Taketoshi, F. Akira., Langmuir 26 (14) (2010) 11628–11630.
[27] B. Feng, J.Y. Chen, S.K. Qi, L. He, J.Z. Zhao, X.D. Zhang., J. Mater. Sci. Mater. Med. 13 (2002) 457–464.
[28] T. Hanawa, M. Ota, Biomaterials 12 (1991) 767–774.
[29] H. Ishizawa, M. Fujnno, M. Igino., J. Biomed. Mater. Res. 29 (1995) 1459–1468.
[30] P. Li, K.J. Degroot, Biomed. Mater. Res. 12 (1993) 1497.
[31] P. Li, K. Degroot, J.T. Kokubo., J. Am. Ceram. Soc 77 (1994) 524–530.
[32] T.K. Sham, M.S. Lazarus., Chem. Phys. Lett. 68 (1979) 426–432.
[33] H.P. Boehm., Discuss. Faraday Soc 52 (1971) 264–275.
[34] B. Feng, J. Weng, B.C. Yang, S.X. Qu, X.D. Zhang., Biomaterials 24 (2003) 4663–4670.
[35] W.V. Vander, H.C. Vander Mei, H.J. Usscher., Langmuir 10 (1994) 1314–1318.
[36] J.Y. Martin, Z. Schwartz, T.W. Hummert, D.M. Schraub, J. Simpson, J.J. Lankford, D.D. Dean, D.L. Cochranand, B.D. Boyan., J. Biomed. Mater. Res. 29 (1995) 389–401.
[37] M. Lampin, R.W. Clerout, C. Legris, MFS-luizard. IBID 36 (1997) 99.